Cross sections of e^--O scattering at intermediate and high energies ($E_i = 8.7-1000$ eV)

K. N. Joshipura
Department of Physics, Sardar Patel University, Vallabh Vidyanagar 388 120, Gujarat, India

P. M. Patel
Department of Physics, V.P. & R.P.T.P. Science College, Vallabh Vidyanagar 388 120, Gujarat, India

(Received 1 February 1993)

Various total cross sections and elastic differential as well as momentum-transfer cross sections for electron scattering by oxygen atoms are calculated for incident energies $E_i = 8.7-1000$ eV. A partial-wave analysis of the local, complex, energy-dependent optical potential yields reliable total cross sections. Discrepancies between theories and experiment exist at low energies, but a reasonable energy-variation picture of various e^--O cross sections emerges. The present total inelastic cross sections are similar to but higher than the recommended total ionization cross sections.

PACS number(s): 34.80.−i

I. INTRODUCTION

There have been several earlier [1–5] as well as recent [6–9] investigations on the scattering of electrons by atomic oxygen in its ground (^3P) state. Elastic-scattering measurements on the e^--O system, done by Williams and Allen [6] are available at low energies, up to 8.7 eV only. There are hardly any experiments on this system at intermediate and high energies, and the theoretical investigations [3,5,8] are also scarce and inadequate. At such energies the e^--O system may be represented reasonably well by a local, complex, and energy-dependent optical potential to treat elastic scattering. However, the main physical effects must be included adequately in the optical potential. Recent compilations of Itikawa and Ichimura [7] on this system are based on, among other things, the calculations of Blaha and Davis [3], in which the polarization effect was not treated adequately. It becomes necessary here to employ different model potentials to account for this effect in the different regions of incident energy. In the present paper, we report, over a wide energy range ($E_i = 8.7-1000$ eV) our theoretical investigations on total elastic cross sections $Q_{\rm el}$, total inelastic cross sections $Q_{\rm inel}$, total (elastic plus inelastic) cross sections Q_T, elastic differential cross sections (DCS), and the momentum-transfer cross sections Q_M for the e^--O scattering. We have tested our results against the background of experimental and other available data. Notably, plenty of reliable data are available on e^--O_2 scattering. We have used the data here to draw conclusions regarding the e^--O system, within the framework of the independent-atom model, at high energies roughly above 100 eV.

II. THEORETICAL MODELS AND CALCULATIONS

We represented all the major interactions of the e^--O scattering through a complex, energy-dependent, optical potential $V_{\rm opt}(r,E_i)$. The real component of the $V_{\rm opt}$ consisted of the static, exchange [10], and polarization potentials, while the imaginary component was in the form of an absorption potential [11]. The target charge density $\rho(r)$ required to express these potentials was calculated through Hartree-Fock (HF) wave functions [12]. Various properties of the oxygen atom which are required in the present calculations are given in Table I.

Detailed expressions of the static, exchange [10], and the absorption [11] potential are omitted here. To account for the polarization effect at intermediate energies ($E_i = 10-50$ eV), we follow the correlation polarization [9,13], or the CP model. In this model the short-range and the long-range terms of the polarization potential are joined at their first crossing point $r = r_0$, such that

$$V_{\rm CP}(r) = \begin{cases} V_{\rm cor}[\rho(r)], & r \le r_0 \\ -\dfrac{\alpha_d}{2r^4}, & r > r_0, \end{cases} \tag{1}$$

where the correlation potential $V_{\rm cor}$ is determined as a density functional (Ref. [13]) and where α_d is the dipole polarizability. This form of the CP potential does not describe the observed features [6] at low energies, as the short-range part $V_{\rm cor}$ turns out to be rather strong [9]. Hence, at 8.7 eV, the lowest energy of our present interest, we adopted the well-known sharp cutoff version

$$V_{\rm pol}(r;r_0) = -\frac{\alpha_d}{2r^4}\{1-\exp[-(r/r_0)^6]\}\ , \tag{2}$$

TABLE I. Properties of atomic oxygen adopted [5,7] in the present work.

1.	Dipole (quadrupole) polarizability α_d (α_q)	5.2 (16.3) a.u.
2.	Mean excitation energy	1.005 hartree
3.	First excitation threshold	9.146 eV
4.	Ionization potential energy	13.618 eV

 ©1993 The American Physical Society

where the cutoff parameter was chosen to be $r_0=2.97a_0$, as determined from Eq. (1) for atomic oxygen. Now, towards high energies the CP model fails to describe the dynamic response of the target to the impinging electron. Hence, we employed the following dynamic polarization potential [5,9] for $E_i > 50$ eV:

$$V_{\rm DP}(r;k)=-\frac{1}{2}\left[\frac{\alpha_d r^2}{(r^2+r_c^2)^3}+\frac{\alpha_q r^4}{(r^2+r_c^2)^5}\right],$$

$$\text{with } r_c=0.375k/\Delta\ . \quad (3)$$

Here, k is the incident momentum, and other parameters of Eq. (3) are given in Table I. Thus, in order to represent polarization effects, we have chosen Eq. (1) at $E_i=10-50$ eV, Eq. (2) at $E_i=8.7$ eV, and Eq. (3) for $E_i > 50$ eV.

In a partial-wave decomposition scheme, the radial Schrödinger equation incorporating $V_{\rm opt}$ was solved by the variable step-size Numerov method, and the complex phase shifts $\delta_l(k)$ were obtained. The step size for radial integrations was varied typically from $0.001a_0$ to $0.05a_0$. The step size and the (large) "matching" distance were so chosen as to achieve the convergence of the phase shifts within 10^{-5} rad. The maximum number of partial waves $l_{\rm max}$ required to compute the present cross sections varied from 20 to 200, depending on E_i. The total elastic cross section $Q_{\rm el}$ and the total inelastic cross section $Q_{\rm inel}$, calculated from $\delta_l(k)$ using the standard expressions [14], yield

$$Q_T=Q_{\rm el}+Q_{\rm inel}\ . \quad (4)$$

Thus, $Q_{\rm inel}$ describes the collective effect of all nonelastic scattering, including ionization processes. The total (elastic plus inelastic) cross section Q_T calculated directly through the optical theorem numerically agrees with that obtained from Eq. (4).

III. RESULTS AND DISCUSSION

Oxygen is an important light open-shell atom with moderate polarizabilities. The present theoretical work gives a reliable picture of its electron-scattering properties in terms of magnitudes and energy dependence. The elastic differential cross section (DCS) of e^--O scattering is shown in Figs. 1, 2, and 3 at representative energies. A comparison with the measured angular distribution of Williams and Allen [6] at 8.7 eV (Fig. 1) shows a good general agreement at intermediate and large angles. Our theoretical values (and also earlier theoretical data) are lower than the measured DCS at small angles ($\theta < 30°$) in the low-energy region. Our calculated phase shifts converge slowly in comparison with those obtained from the measured DCS (Ref. [6]), and hence the small-angle discrepancy. The approximate exchange and the CP potentials also contribute to the same. At a typical intermediate energy of 50 eV (Fig. 2), the theoretical DCS show a deep minimum around 90°. In Fig. 2 our complex-optical-potential (COP) results differ somewhat from our real-potential (RP) results, which ignore the absorption effects. At 50, 100, and 500 eV (Figs. 2 and 3),

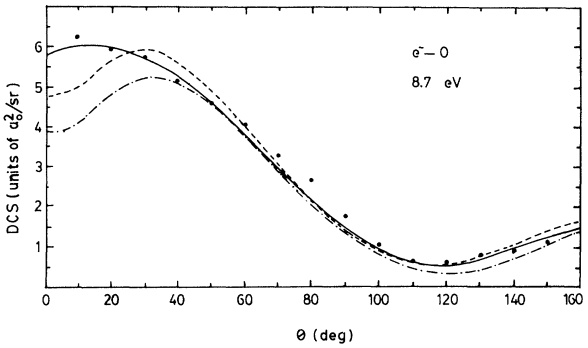

FIG. 1. DCS of e^--O scattering at 8.7 eV: ●, measurements of Williams and Allen [6]; ——, from statistical phase shifts of these measurements; — — — —, present results with $V_{\rm pol}(r;r_0)$; and –·–·, present results with $V_{\rm CP}$.

the theoretical results of Ref. [3] are qualitatively similar to ours, but they are lower than ours at small angles, because of their [3] neglect of polarization beyond the partial wave $l=3$. At high energies, e.g., 500 eV, the polarization effects are significant only at small angles below 20° or so. Beyond this, the present and the previous [3] theories are quite similar. Hence, in Fig. 3, the two 500-eV DCS's are virtually identical, except for 0°–20°. The dynamic polarization potential is reasonably well suited at high energies. Now, in Fig. 3, the present DCS's at

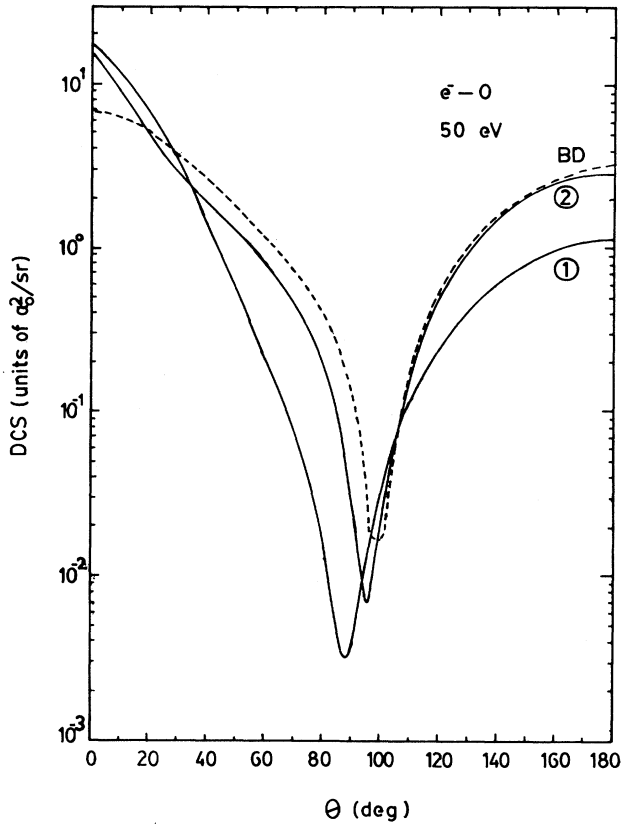

FIG. 2. 50 eV: Curve (1), present COP results; Curve (2), present RP results; and – – – –, Blaha and Davis, Ref. [3].

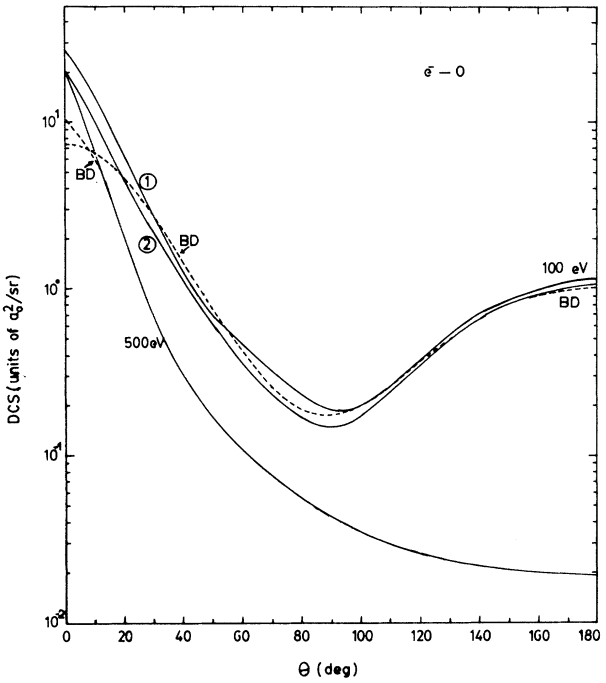

FIG. 3. Upper curves, 100 eV; Lower curve, 500 eV. Curve (1), present results with the dynamic polarization potential; curve (2), present results with V_{CP}; ----, Ref. [3].

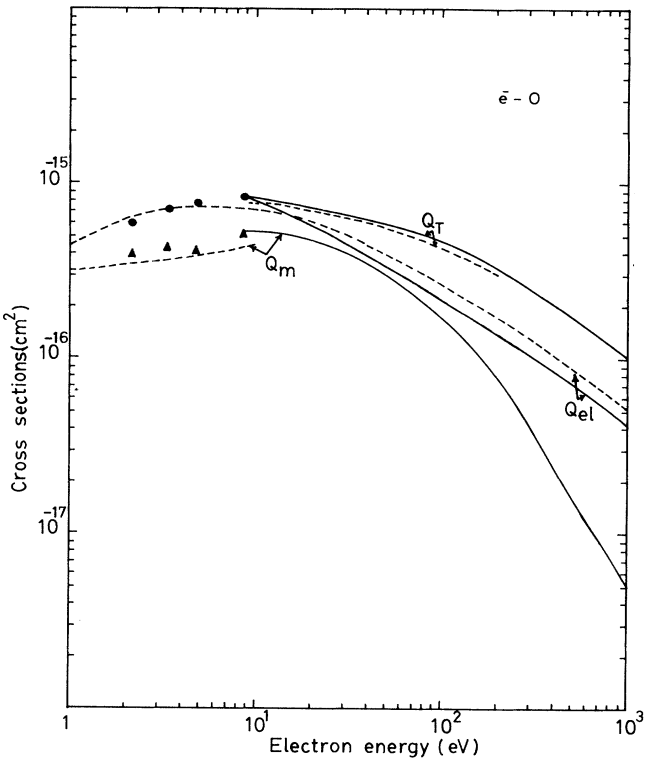

FIG. 4. Various cross sections of e^--O scattering as functions of energy: ——, present; ----, Itikawa and Ichimura [7]; ● and ▲, measurements of Williams and Allen [6].

100 and 500 eV are exhibited in the real potential (V_{RP}) only. Towards high energies, the absorption potential of Ref. [11], adapted for e^--O scattering, shows a rather excessive loss of flux in the inelastic channels, at small r. The resulting large-angle DCS's in V_{opt} are much lower. This was also observed by Jain [15] for CH_4. Now the momentum-transfer cross section (MTCS) Q_M, being more sensitive to the large-angle DCS, also get reduced correspondingly. In Fig. 4 the exhibited Q_M values at $E_i \geq 100$ eV are those obtained in V_{RP} only. Notably, the e^--O_2 cross sections based on the RP-DCS of e^--O scattering show a good accord with experiments (Ref. [8] and references therein).

Our Fig. 4 depicts various total cross sections of e^--O scattering as functions of energy. Also included are the previous theoretical [7] and the experimental [6] results at low energies, in order to afford a complete energy-variation picture. We have $Q_T = Q_{el}$ for $E_i \leq 9.146$ eV (see Table I) in the present case. Our calculated value of Q_T (or Q_{el}) at 8.7 eV agrees very well with the experiment [6]. Beyond this energy, our values of Q_{el} are slightly lower than the published data [7], since our calculations also include the effect of inelastic scattering [Eq. (4)]. The cross sections Q_T and Q_{el} exhibit a broad maximum centered around 10 eV or so. The total inelastic cross section Q_{inel} (not shown) has a peak between 50 and 100 eV. It is qualitatively similar to but higher than the recommended total e^--O ionization cross sections given in Ref. [7].

The momentum-transfer cross section Q_M (Fig. 4) peaks around 10 eV and decreases rapidly, since the backscattering is subdued at high energies. The difference between experiment and theory is larger for Q_M than for Q_{el}, below about 10 eV. The present local potentials are inadequate at these energies.

At high energies, on the other hand, an indirect support of our calculations is offered by an independent-atom model [16] connecting e^--O_2 and e^--O cross sections. In this model we can formulate [9] an additivity rule [17] expressing the molecular cross section Q_T as an incoherent sum of the Q_Ts of the constituent atoms. Thus at 300 eV the present $Q_T = 2.57 \times 10^{-16}$ cm^2 for atomic oxygen, when multiplied by 2, is consistent with the experimental result [18] for O_2 molecules, viz., 4.9×10^{-16} cm^2. The measured data [18] on O_2 indirectly confirm our results on the oxygen atom, above 100 eV or so. The present values of Q_{el} for e^--O scattering differ from those of Ref. [8] in which exchange and absorption effects are not considered. At intermediate energies all our total cross sections are expected to be better than the previous results. Towards low energies, a discrepancy exists between theory and experiment, especially in the small-angles DCS's, but the work presented here still offers a reasonable energy-variation picture of various e^--O cross sections.

[1] G. Sunshine, B. B. Aubrey, and B. Bederson, Phys. Rev. **154**, 1 (1967).
[2] L. D. Thomas and R. K. Nesbet, Phys. Rev. A **11**, 170 (1975).
[3] M. Blaha and J. Davis, Phys. Rev. A **12**, 2319 (1975).
[4] B. R. Tambe and R. J. W. Henry, Phys. Rev. A **13**, 224 (1976).
[5] Y. D. Kaushik, S. P. Khare, and D. Raj, Indian J. Pure Appl. Phys. **20**, 538 (1982).
[6] J. F. Williams and L. J. Allen, J. Phys. B **22**, 3529 (1989).
[7] Y. Itikawa and A. Ichimura, J. Phys. Chem. Ref. Data **19**, 637 (1990).
[8] D. Raj, Phys. Lett. A **160**, 571 (1991).
[9] K. N. Joshipura and P. M. Patel, Pramana **38**, 329 (1992); **39**, 293 (1992).
[10] S. Hara, J. Phys. Soc. Jpn. **22**, 710 (1967).
[11] G. Staszewska, D. Schwenke, D. Thirumalai, and D. G. Truhlar, Phys. Rev. A **28**, 2740 (1983).
[12] E. Clementi and C. Roetti, At. Data Nucl. Data Tables **14**, 177 (1974).
[13] N. T. Padial and D. W. Norcross, Phys. Rev. A **29**, 1742 (1984).
[14] C. J. Joachain, *Quantum Collision Theory* (North-Holland, Amsterdam, 1983), p. 105.
[15] Ashok Jain, Phys. Rev. A **34**, 3707 (1986).
[16] N. F. Mott and H. S. W. Massey, *Theory of Atomic Collisions* (Oxford, Clarendon, 1987), p. 197.
[17] See, e.g., *Electron Impact Ionization,* edited by S. M. Younger and T. D. Mark (Springer, New York, 1985), p. 1.
[18] M. S. Dababneh, Y. F. Hsieh, W. E. Kaupilla, C. K. Kwan, S. J. Smith, T. S. Stein, and M. N. Uddin, Phys. Rev. A **38**, 1207 (1988).